Lab on a Chip

Accepted Manuscript

ROYAL SOCIETY OF CHEMISTRY

www.rsc.org/loc

Cite this: DOI: 10.1039/c0xx00000x

www.rsc.org/xxxxxx

COMMUNICATION

Osmotic pressure-triggered cavitation in microcapsules

Luoran Shang,[a] Yao Cheng,[a] Jie Wang,[a] Yunru Yu,[a] Yuanjin Zhao,[*a] Yongping Chen[*b] and Zhongze Gu[*a]

Received (in XXX, XXX) Xth XXXXXXXXX 20XX, Accepted Xth XXXXXXXXX 20XX
DOI: 10.1039/b000000x

Cavitation system was found in solid microcapsules with a membrane shell and a liquid core. When simply treating these microcapsules with hypertonic solutions, cavitation could be controllably triggered without special equipment or complex operations. The cavitation-formed vapor bubble was fully entrapped within the microcapsules, thus providing an advantageous method for fabricating encapsulated microbubbles with controllable dimensions and functional ingredients.

When the pressure acting on a liquid is decreased beyond a critical tension, the liquid can form vapor bubbles spontaneously by aggregating submerged small gas nuclei to relatively large volumes. This phenomenon is known as cavitation.[1-3] Cavitation events exist widely in nature and have attracted significant attention in many diverse fields of science and engineering because of their distinct features. For example, heterogeneous nucleation plays an important role both in plant xylem for the ascent of sap[4-5] and in the annulus cells of sporangia for the ejection of spores.[6-7] This has motivated many studies to investigate cavitation systems based on free or confined liquids.[8-14] However, most of the current strategies for triggering cavitation require elaborate micro/nanostructure design and employ focused laser pulses or acoustic waves,[15-20] which are expensive and demanding in operation. In addition, the studies of these cavitation events have focused mainly on their formation mechanisms, while little attention has been given to exploiting their potential value in applications. Thus, novel cavitation systems with simple triggering mechanisms and potential applications are still sought.

In this paper, we present our finding about an osmotic pressure-triggered cavitation system with the desired features based on microfluidic microcapsules. Because of the excellent ability to control the structures of the final emulsion templates, microfluidic techniques have emerged as a promising and versatile method for generating monodisperse microcapsules and other types of particles for different applications.[21-26] However, the potential value of these particles in the construction of cavitation system remains unexplored. Therefore, we have here employed capillary microfluidics to generate solid microcapsules with a semipermeable membrane shell and a liquid core. By simply treating these microcapsules with hypertonic solutions, which present an osmotic pressure to induce outward flux of water across the spherical shell and to cause gas supersaturation in the core, negative liquid pressure was established suddenly and cavitation could be controllably triggered in the microcapsules without special equipment or complex operation, as outlined in **Figure 1**. More importantly, the cavitation-formed vapor bubble is fully entrapped within the microcapsule; this provides an advantageous method for fabricating encapsulated microbubbles. In contrast to the current reported methods for fabricating microbubbles by using gas-filled emulsions as templates, which suffer from uncontrollable coalescence, rupture, and size distribution,[27-33] the proposed approach could greatly improve the stability and tunability of the bubble generation process. In addition, a series of multicore and functional microbubbles could be derived using our approach by treating different microcapsule templates.

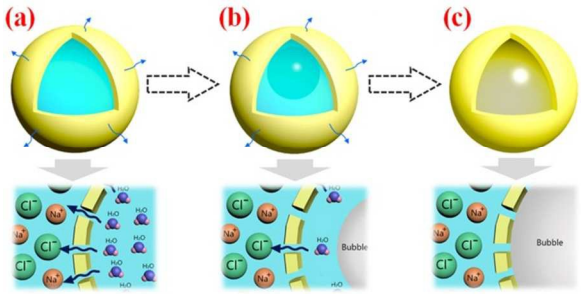

Fig. 1 Schematic illustration of the semipermeable microcapsule cavitation system: when the microcapsule was subjected to a hypertonic environment, the osmotic pressure induced outward flux of the inner water caused local gas supersaturation, and thus triggered cavitation. (a) The initial water-filled microcapsule template; (b) the occurrence of cavitation; (c) the ultimate encapsulated microbubble. Below each figure, there is a corresponding details view showing the osmotic pressure-triggered cavitation mechanism.

To create the solid microcapsules with a semipermeable membrane shell and a liquid core, we generated double emulsions in microfluidic devices and used the emulsions as templates for the final microcapsules. In a typical experiment, we first prepared water in oil in water (W/O/W) double emulsions using a glass capillary microfluidic device, as illustrated in **Figure 2a**. The device was integrated by coaxially assembling three cylindrical capillaries, through which the inner, middle, and outer phases were introduced respectively to form a sequential co-flow regime. The inner and outer phases were both aqueous surfactant solutions, while the middle oil phase was a photocurable ethoxylated trimethylolpropane triacrylate (ETPTA) resin with

1% 2-hydroxy-2-methylphenylpropanone photoinitiator. When the three phases were forced to flow in the microfluidic channels, the inner aqueous flow was sheared into droplets by the middle oil stream, and the middle flow containing inner droplets was broken up by the outer aqueous stream at the middle capillary orifice, thus consecutively generating W/O/W double emulsions, as recorded in **Figure 2b**. Finally, the photocurable shells of the emulsions were solidified downstream upon UV irradiation. In contrast to bulk emulsification methods, the double emulsions and the resultant microcapsules in a microfluidic device are made by precisely fabricating one drop at a time. This process results in highly monodisperse emulsions and microcapsules (**Figure S1**). In addition, by adjusting the flow rates of the three phases, the overall sizes of the microcapsules and their encapsulated core droplets could be controlled, as shown in **Figure 2c–2e** and **Figure S2**.

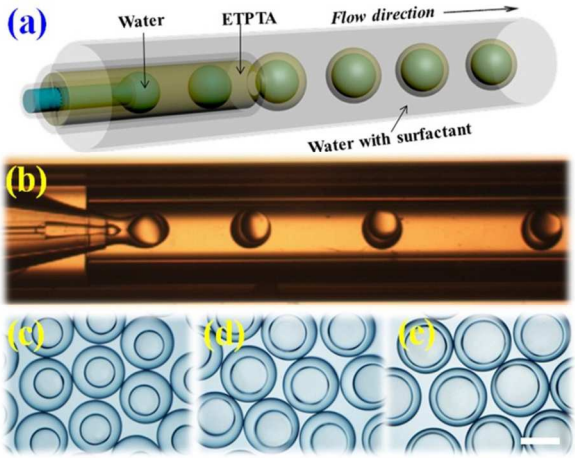

Fig. 2 Microfluidic fabrication of double emulsions and microcapsules. (a, b) Schematic diagram and real-time image of the glass microfluidic fabrication of the double emulsions; (c-e) microscope photographs of the three kinds of monodisperse microcapsules with different sizes. Scale bar is 300 μm.

The as-prepared microcapsules were then immersed in saturated sodium chloride (NaCl) solutions. As the shell of each microcapsule is a semipermeable ETPTA resin membrane, which is permeable to water and impermeable to Na^+ and Cl^- ions, interior water in the core of the microcapsules is drawn out because of the osmotic pressure difference across the ETPTA shell. In our system, the osmotic pressure difference across the shell can be estimated by:[34]

$$\Pi = (2c_{NaCl} + \Pi_{out} - \Pi_{in}) \times N_A k_B T, \quad (1)$$

where c_{NaCl} is the concentration of the NaCl solution, and Π_{in} and Π_{out} are the fluid osmolarities inside and outside the microcapsules in the absence of NaCl, respectively. N_A is Avogadro's constant, and k_B is Boltzmann's constant. T is the thermodynamic temperature (in this case, T ≈300 K). Thus, the osmotic pressure increased with the NaCl concentration. The responses of the microcapsules under a given osmotic pressure were related to their morphology. It has been reported in many papers that microcapsules with soft shells will buckle under osmotic pressure or other external forces.[34, 35] However, as far as we know, the response of rigid shell microcapsules under osmotic pressure or other external forces has not been investigated. We thought that this system would also allow the generation of negative pressure (tension) in the water cores because of the drawing-out of water by high external osmotic pressure. Tension would increase slowly as the water was continuously drawn out, and the water in the microcapsules would experience a stretched, metastable state. When the liquid pressure in the cores decreased to a critical value, spontaneous cavitation in the metastable water should result in the creation of a bubble, thus relaxing their tension.[11]

To confirm our hypothesis, we monitored the evolution process of the ETPTA microcapsules in a saturated NaCl solution using an optical microscope and sequentially captured images after time intervals, as shown in **Figure 3**. The same phenomenon as others reported,[34, 35] the thin-shell (in this case, less than 30μm for the microcapsules with the size of 450μm) buckled shortly after immersion in the saturated hypertonic solution, and a dimple appeared on the shell and deepened over time (**Figure 3a**). Finally, most of the water in the core was drawn out, and the shells of the microcapsules folded inwards and deformed (**Figure S3a**). It was worth noting that in some cases, the thin-shell microcapsules would suddenly burst and form an indentation because of brittle rupture (**Figure S3b–3d**).

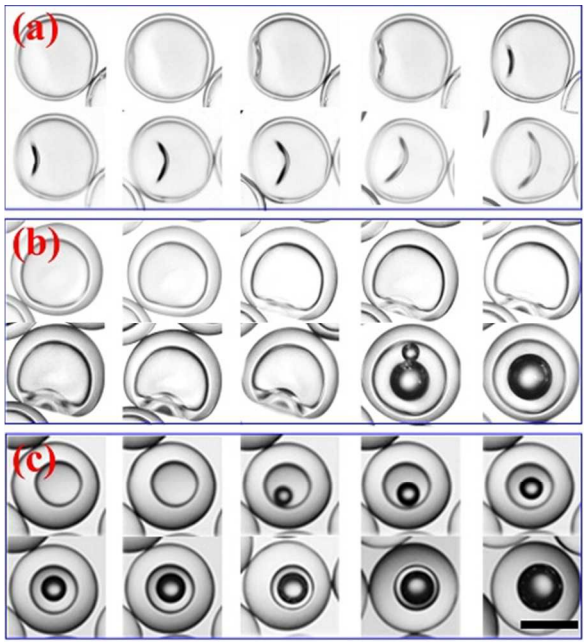

Fig. 3 The three distinct evolution patterns of the microcapsules under a saturated hypertonic solution. (a) Microcapsules with a thin shell buckled immediately and the dimple deepened over time, without bubble generation in the whole process; (b) microcapsules with a medium-thickness shell buckled firstly and a huge bubble emerged suddenly; (c) microcapsules with a thick shell did not buckle, but still with a bubble appeared and grew. Scale bar is 300 μm.

When the thickness of the ETPTA shells was increased to a medium level (between 30 and 100 μm for the microcapsules with the size of 450μm), the water in the cores could still be drawn out. Initially, these microcapsules also buckled like the thin-shell ones in the saturated hypertonic solution (**Figure 3b**), although the buckling could only begin at the thinnest spot of the

shells and the drawing-out process was much slower because of the extended semipermeable channels. However, with the drawing of water from the cores, the buckling process slowed and even stopped. This was because the elastic counterforce increased with the degree of deformation of the shell, until it reached a balance with the osmotic pressure. Then suddenly, a relatively huge bubble emerged in the core, indicating the occurrence of cavitation. So far as we know, this type of cavitation inside microcapsules is the first examples. The cavitation phenomenon should be ascribed to the continuing outward flux of water after the balance, which contributed to a sudden reduction in the internal pressure. Such negative pressure triggered the cavitation in the microcapsule. As the bubble grew, the microcapsules returned to their original spherical shapes because of the release of the negative pressure in their inner cores. This pattern of the microcapsule buckling and the bubble occurrence process was recorded in **movie S1**. It should be noted that the speed of the microcapsules buckling accelerated with the increase of NaCl concentration (also the increase of osmotic pressure).[35] In this study, saturated NaCl solution was employed to ensure that the osmotic pressure is high enough for triggering cavitation.

We further increased the shell thickness of the ETPTA microcapsules and investigated their response under the same saturated hypertonic solution. It was found that the thick shell (more than 100 μm for the microcapsules with the size of 450μm) was more rigid and the microcapsules could sustain their intact spherical shape without deformation under the high osmotic pressure. With the drawing of water from the cores, negative pressure enhanced gradually, and the water in the cores approached a stretched, metastable state. When the negative pressure decreased to a critical value, spontaneous cavitation by forming a bubble in the water core of the microcapsule was also triggered suddenly to relax the tension, as shown in **Figure 3c**. In addition, under the hypertonic osmotic pressure, the nucleated bubble grew continuously until it filled the entire inner core of the microcapsule (**movie S2**).

To demonstrate the potential value of our cavitation system, it was employed for bubble generation. In contrast to conventional bubble fabrication strategies using sonication or high-shear emulsification, which often result in microbubbles with broad size distributions, our method could generate highly monodisperse microbubbles, as shown in **Figure 4**. Although monodispersity of microbubbles has been demonstrated several times in other studies using microfluidic emulsification technologies, these methods still suffered from uncontrollable coalescence or rupture because of density disparity during the bubble generation, which hindered the bubble encapsulation efficiency. Moreover, in the microfluidic approaches, the gas-liquid surface tension is much larger than that of liquid–liquid systems, such that the interfacial actions mainly influence the liquid phase, making it difficult to manipulate bubble size. In comparison, the microbubbles in our system were derived from liquid cores, which were encapsulated in solid shells; thus, the bubble generation processes were very stable and were not affected by a density disparity. In addition, the sizes of the generated microbubbles could easily be controlled by using different time for treating the microcapsule templates (**Figure S4**); thus, our method could achieve monodisperse microbubbles of different sizes (**Figure 4b–4f**). These microbubbles maintained their size and morphology for several weeks in water solution.

A notable feature of the osmotic pressure-triggered microcapsule cavitation system was its ability to generate multicore bubbles. Such bubbles are difficult to achieve using other methods because the bubble cores tend to coalesce. However, in our method, microcapsules with multiple, stable liquid cores were first fabricated by changing the flow rates in the microfluidics (**Figure S5**). These multiple core microcapsules were then used as templates for bubble generation by forming the cavitation in each core (**Figure 4g–4l**). As these cores were separated by the solid ETPTA resin, the coalescence of the formed microbubbles in a single microcapsule was avoided. The interaction between the microbubbles and the acoustic wave was investigated through acoustic imaging experiments (**Figure S6**). It was indicated that the ultrasonic contrast signal could be enhanced by our microbubbles. However, it should note that only when the shell membrane of the microbubbles was replaced by biocompatible and biodegradable polymers, they can find the practical *in vivo* applications.

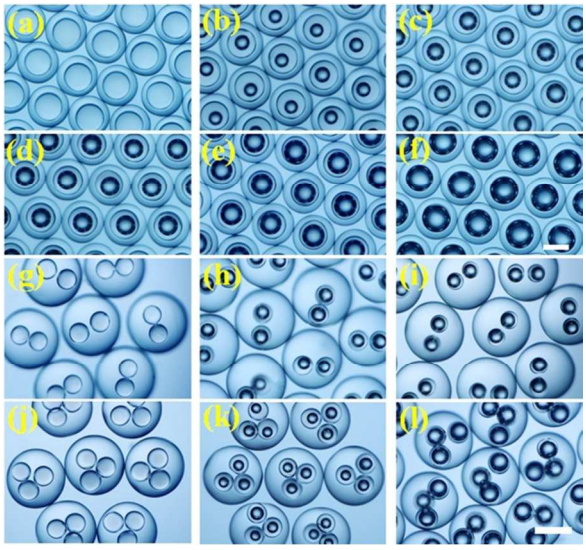

Fig. 4 Microscope photographs of the cavitation derived microbubbles in microcapsules. (a) the initial single-core liquid-filled microcapsules; (b-f) monodisperse microbubbles in polymeric shells under different time of hypertonic solution treating. (g-i) cavitation occurrence process in double-core microcapsules and the generation of double-core microbubbles; (j-l) cavitation occurrence process in triple-core microcapsules and the generation of triple-core microbubbles. Scale bars are 300 μm.

To impart additional functionality to the microbubbles, we also employed nanoparticle-tagged microcapsules as the templates for the microbubbles generation. For instance, magnetic microbubbles can be fabricated by incorporating Fe_3O_4 or Fe_2O_3 nanoparticles in the water cores or ETPTA shells during microcapsule generation. When the magnetic nanoparticles were in the water cores of the microcapsules (**Figure 5a-5c**), cavitation bubbles could still appear in the cores accompanying the drawing out of the water by the saturated hypertonic solution (**Figure 5d-5f**). During this process, the hydrosoluble magnetic nanoparticles could only stay in the residual water of the cores. With the

complete drawing-out of the water from the cores, these nanoparticles formed a uniform solid crystal layer on the inner surface of the microcapsule shell, as confirmed by confocal microscope in **Figure 5g-5h**. This should ascribe to the omnibearing water extraction across the ETPTA shells during the treatment. Thus, functional microbubbles with both a magnetic nanoparticle crystal layer and a polymer shell layer were achieved by our method. In addition, by dispersing high concentrations of magnetic nanoparticles in the ETPTA shells, the resultant microbubbles gained the function of controllable motion (**Figure 5i-5j**). Such nanoparticle-tagged functional microbubbles have been sought in many different areas field, respectively.

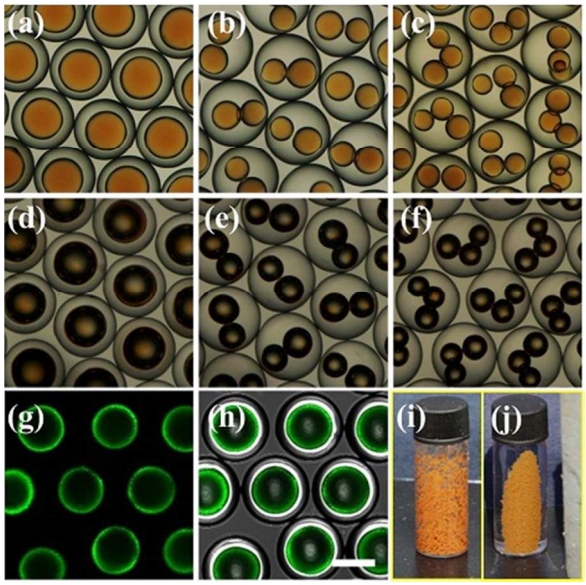

Fig. 5 Nanoparticles-tagged microcapsules and the derived nanoparticles-tagged microbubbles. (a-c) microscopic photograph of liquid-filled microcapsules with single, double, and triple magnetic cores, respectively; (d-f) the corresponding microbubbles with both magnetic nanoparticles crystal layer and polymer shell layer derived from (a-c); (g-h) the CLSM images of (d); (i-j) controllable motion of microbubbles with magnetic nanoparticles-tagged ETPTA shells. These magnetic particles were uniformly distributed and pulled to one side of a vial before (i) and after (j) applying a magnet field, respectively. Scale bar is 300μm.

In conclusion, we have shown a novel cavitation system in solid microcapsules with a semipermeable membrane shell and a liquid core. Without special equipment or complex operations, the cavitation was controllably triggered by simply treating these microcapsules with hypertonic solutions that provide an osmotic pressure to induce outward flux of water across the spherical shell and to cause gas supersaturation in the cores. The cavitation-formed vapor bubble was fully entrapped within the microcapsule, which provided an advantageous manner for fabricating encapsulated microbubbles. Our method greatly improves the stability and tunability of the bubble generation process, and thus overcomes the restrictions of uncontrollable coalescence, rupture, and size distribution in microbubble generation using other approaches. We have also demonstrated that a series of multicore and functional microbubbles could be achieved using our approach by treating different microcapsule templates. We expect that our method and the resultant microbubbles will find important biomedical applications.

Acknowledgments

This work was supported by the National Science Foundation of China (Grant Nos. 21473029, 91227124 and 51522302), the NASF Foundation of China (Grant No. U1530260), the National Science Foundation of Jiangsu (Grant No. BK20140028), the Science and Technology Development Program of Suzhou (Grant No. ZXG2012021), the Research Fund for the Doctoral Program of Higher Education of China (20120092130006), and the Program for New Century Excellent Talents in University.

Notes and references

[a] *State Key Laboratory of Bioelectronics, School of Biological Science and Medical Engineering, Southeast University, Nanjing 210096, China. Fax: +86 25-83795635; Tel: +86 25-83795635; E-mail: yjzhao@seu.edu.cn; gu@seu.edu.cn*
[b] *School of Energy and Environment, Southeast University, Nanjing 210096 , China. E-mail: ypchen@seu.edu.cn;*

1 P. G. Debenedetti, *Nat. Phys.* 2013, **9**, 7.
2 C. H. Duan, R. Karnikb, M. C. Lua, A. Majumdara, C. Duan, R. Karnik, M. C. Lu, and A. P. Majumdar, *P. Natl. Acad. Sci. USA* 2012, **109**, 3688.
3 D. G. Shchukin, E. Skorb, V. Belova, and H. Möhwald, *Adv. Mater.* 2011, **23**, 1922.
4 T. D. Wheeler and A. D. Stroock, *Nature* 2008, **455**, 208.
5 P. Ball, *Nat. Mater.* 2014, **13**, 922.
6 X. Noblin, N. O.Rojas, J. Westbrook, C. Llorens, M. Argentina and J. Dumais, *Science* 2012, **335**, 1322.
7 X. Chen, L. Mahadevan, A. Driks and O. Sahin, *Nat. Nanotechnol.* 2014, **9**, 137.
8 M. Ashokkumar, M. Hodnett, B. Zeqiri, F. Grieser and G. J. Price, *J. Am. Chem. Soc.* 2007, **129**, 2250.
9 R. P. Taleyarkhan, C. D. West, J. S. Cho, R. T. Lahey Jr., R. I. Nigmatulin and R. C. Block, *Science* 2002, **295**, 1868.
10 M. E. M. Azouzi, C. Ramboz, J. F. Lenain and F. Caupin, *Nat. Phys.* 2013, **9**, 38.
11 O. Vincent, P. Marmottant, S. R. Gonzalez-Avila, K. Ando and C-D. Ohl, *Soft Matter*, 2014, **10**, 1455.
12 M. F. Chung, K. J. Chen, H. F. Liang, Z. X. Liao, W. T. Chia, Y. N. Xia and H. W. Sung, *Angew. Chem.* 2012, **124**, 10236.
13 N. Bremond, M. Arora, C. D. Ohl and D. Lohse, *Phys. Rev. Lett.* 2006, **96**, 224501.
14 H. S. Chen, J. Li, W. Z. Zhou, E. G. Pelan, S. D. Stoyanov, L. N. Arnaudov and H. A. Stone, *Langmuir* 2014, **30**, 4262.
15 P. A. Quinto-Su, *Nat. Commun.* 2014, **5**, 5889.
16 Z. Y. Lu, W. Zhu, X. Y. Yu, H. C. Zhang, Y. J. Li, X. M. Sun, X. W. Wang, H. Wang, J. M. Wang, J. Luo, X. D. Lei and L. Jiang, *Adv. Mater.* 2014, **26**, 2683.
17 J. Li, H. S. Chen, W. Z. Zhou, B. Wu, S. D. Stoyanov and E. G. Pelan, *Langmuir* 2014, **30**, 4223.
18 G. Lajoinie, E. Gelderblom, C. Chlon, M. Böhmer, W. Steenbergen, N. de Jong, S. Manohar and M. Versluis, *Nat. Commun.* 2014, **5**, 3671.
19 H. Okumura and S. G. Itoh, *J. Am. Chem. .Soc.* 2014, **136**, 10549.
20 Z. G. Li, S. Xiong, L. K. Chin, K. Ando, J. B. Zhang, and A. Q. Liu, *Lab Chip.* 2015, **15**, 2158.
21 L. Y. Chu, A. S. Utada, R. K. Shah, J. W. Kim and D .A. Weitz, *Angew. Chem. Int. Ed.* 2007, **46**, 8970.

22 Y. J. Zhao, H. C. Shum, H. S. Chen, L. L. A. Adams, Z. Z. Gu and D. A. Weitz, *J. Am. Chem. Soc.* 2011, **133**, 8790.

23 T. T. Kong, J. Wu, K. W. K. Yeung, M. K. T. To, H. C. Shum and L. Q. Wang, *Biomicrofluidics* 2013, **7**, 044128.

24 L. Zhang, Q. Feng, J. L. Wang, J. S. Sun, X. H. Shi and X. Y. Jiang, *Angew. Chem. Int. Ed.* 2015, **54**, 3952.

25 L. R. Shang, Y. Cheng, J. Wang, H. B. Ding, F. Rong, Y. J. Zhao and Z. Z. Gu, *Lab Chip* 2014, **14**, 3489.

26 Y. Cheng, F. Y. Zheng, J. Lu, L. R. Shang, Z. Y. Xie, Y. J. Zhao, Y. P. Chen and Z. Z. Gu, *Adv. Mater.* 2014, **26**, 5184.

27 J. D. Wan, A. Bick, M. Sullivan and H. A. Stone, *Adv. Mater.* 2008, **20**, 3314.

28 E. Stride and M. Edirisinghe, *Soft Matter* 2008, **4**, 2350.

29 J. I Park, D. Jagadeesan, R. Williams, W. Oakden, S. Chung, G. J. Stanisz and E. Kumacheva, *ACS Nano* 2010, **4**, 6579.

30 T. Brugarolas, D. S. Gianola, L. Zhang, G. M. Campbell, J. L. Bassani, G. Feng and D. Lee, *ACS Appl. Mater. Inter.* 2014, **6**, 11558.

31 A. Abbaspourrad, W. J. Duncanson, N. Lebedeva, S. H. Kim, A. P. Zhushma, S. S. Datta, P. A. Dayton, S. S. Sheiko, M. Rubinstein and D. A. Weitz, *Langmuir* 2013, **29**, 12352.

32 X. Q. Gong, W. J. Wen and P. Sheng, *Langmuir* 2009, **25**, 7072.

33 K. S. Huang, Y. S. Lin, W. R. Chang, Y. L. Wang and C. H. Yang, *Molecules* 2013, **18**, 9594.

34 S. S. Datta, S. H. Kim, J. Paulose, A. Abbaspourrad, D. R. Nelson and D. A. Weitz, *Phys. Rev. Lett.* 2012, **109**, 134302.

35 S. H. Kim, T. Y. Lee and S. S. Lee, *Small* 2014, **10**, 1155.

TOC

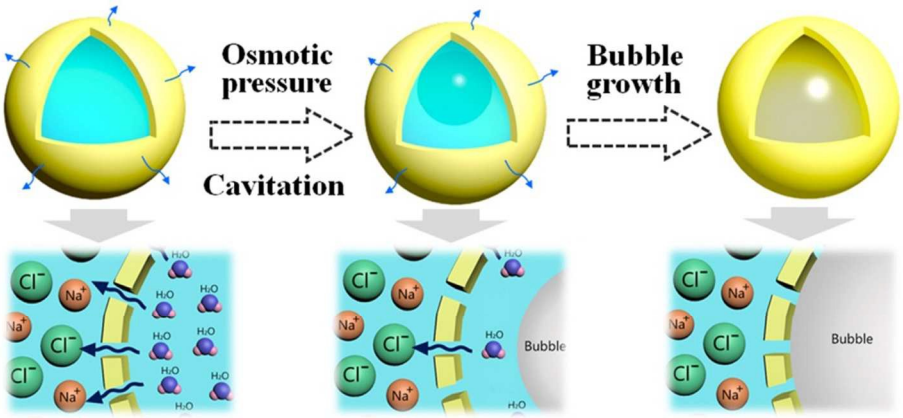

Cavitation was found in solid microcapsules with a membrane shell and a liquid core by treating these microcapsules with hypertonic solutions.